ELECTRICAL PROPERTIES OF NITROGEN RF-SPUTTERED SILICON NITRIDE THIN FILMS: EFFECTS OF GOLD ELECTRODES*

S.A. Awan, R.D. Gould

Thin Films Laboratory, Electronic Engineering Group, Department of Physics, School of Chemistry and Physics, Keele University, Keele, Staffs. ST5 5BG, U.K.

Received 4 December 2002 in final form 18 May 2003, accepted 24 May 2003

Silicon nitride films are widely used in VLSI fabrication due to their high breakdown strength and resistivity. A major topic of interest in this material is the origin of Poole-Frenkel emission which is frequently observed, and typically attributed to centres associated with Si-N bonds. However, in films with aluminium electrodes, prepared by RF magnetron sputtering and using nitrogen as the sputtering gas to ensure stoichiometry, Poole-Frenkel conductivity was absent. In the present work similar films were prepared, but with gold electrodes. Capacitance measurements suggested that the Au electrodes provide ohmic contacts to the silicon nitride films, and that the relative permittivity $\varepsilon_r \sim 6.8$, slightly higher than is the case with Al electrodes. At low DC voltages Ohm's law was obeyed, followed by Poole-Frenkel conductivity with coefficient $\beta \sim 1.95 \times 10^{-5}$ eV $\mathrm{m}^{1/2}$ $\mathrm{V}^{-1/2}$, in contrast to films with Al electrodes. For voltages exceeding 2 V electroforming and differential negative resistance behaviour were observed, as in many thin film insulators having certain noble metal electrodes. The AC conductivity was frequency dependent with index s in the range 0.83 - 1.31. Frequency and temperature variations were typical of a carrier hopping process with an estimated density of localised states $N \sim 10^{24}$ m^{-3}. Carrier activation energies were in the range 0.006 - 0.1 eV, further indicating the presence of hopping conductivity. The dependences of capacitance and loss tangent were consistent with an existing model of dielectric behaviour in sandwich samples having ohmic contacts. It was concluded that the Poole-Frenkel conductivity was associated with centres originating from the Au electrodes, and not from the Si-N bonds.

PACS: 73.40.Rw; 73.50.Fq; 73.61.Ng; 77.55.+f

1 Introduction

Dielectric films play an integral rôle in nearly every semiconductor device and integrated circuit. Silicon nitride (Si_3N_4 if stoichiometric or SiN_x if non-stoichiometric) is used particularly in the areas of diffusion masking, isoplanar processing, gate dielectrics and, most importantly, as an active charge storage insulator for non-volatile memory transistors [1]. Silicon nitride has been used in integrated circuits for several decades [2], is an important material in silicon and III-V device technology [3,4], can be used in antireflecting (AR) coatings in solar cells [5,6], is an

*Presented at Workshop on Solid State Surfaces and Interfaces III,Smolenice, Slovakia, November 19 – 21, 2002.

effective alkali barrier and also protects germanium surfaces from harsh environmental conditions. Si_3N_4 coatings enhance infrared (IR) transmission in germanium in the lower wavelength range [7] and SiN_x films deposited by plasma-enhanced chemical vapour deposition (PECVD) at temperatures below 400 ° C are widely used for encapsulation purposes in integrated circuits [8].

Thin films of silicon nitride are used as gate dielectrics in hydrogenated amorphous silicon thin film transistors (TFTs) [3], and are important in metal-insulator-semiconductor (MIS) inversion layer solar cells as AR and passivation coatings [9,10]. Its use is also becoming increasingly important for the passivation of compound semiconductor materials such as InSb and GaAs [11]. Its high relative permittivity and resistance against migration of alkaline ions represent some of its most significant advantages over SiO_2 [12]. It is an attractive candidate as an advanced dielectric in future generations of ultra-large-scale integration (ULSI) devices [13] and also has many other applications in microelectronics, optoelectronics, optics, and hard surface coatings [14].

Silicon nitride films are usually deposited either by low-pressure chemical vapour deposition (LPCVD) [15] for Si_3N_4 or by plasma-enhanced chemical vapour deposition (PECVD) [16] for SiN_x. These processes took place at temperatures of 800 ° C and 300 ° C respectively [15,16]. Thus LPCVD is used when the stoichiometric nitride Si_3N_4 is essential, whereas PECVD is generally preferred for passivation when the high temperatures of LPCVD would lead to damage of the substrate.

RF magnetron sputtering has some advantages over methods such as PECVD. In PECVD the gases in the reaction normally contain water vapour and hydrogen which can adversely affect the quality of the films [17]. Recently the present authors have investigated radio frequency (RF) magnetron sputtered Si_3N_4 films in the Al-Si_3N_4-Al sandwich configuration [18] where stoichiometry was preserved by the use of a stoichiometric Si_3N_4 target and N_2 as the sputtering gas. Trap density values were similar to those for samples prepared by the CVD techniques, and the mobility and conductivity values were very low, indicating that magnetron sputtering may be a viable technique in device fabrication. However, these films exhibited space-charge-limited conductivity (SCLC) rather than the Poole-Frenkel conductivity normally observed [16,19-22], suggesting that Poole-Frenkel conductivity is not associated solely with the presence of Si-N bonds. In the present work these measurements were extended to samples having Au electrodes in order to probe the effect of the electrode material on the conductivity; furthermore in addition to direct current (DC) measurements to determine the permittivity and the nature of the contact, current density-voltage measurements have been performed to determine the dominant conduction process. Since the dielectric properties of this material are rarely reported [14], in the present work alternating current (AC) measurements have also been made, including measurements of the conductivity, capacitance and loss tangent as functions of frequency and temperature.

2 Experimental details

The films were deposited by RF magnetron sputtering at a frequency of 13.56 MHz in a CVC 601 sputtering system using N_2 as the sputtering gas. Deposition took place at a discharge power and pressure of 100 W and 0.53 Pa respectively. The Si_3N_4 target (Testbourne) was of purity 99.9%; it was circular, of diameter 76 mm and thickness 6 mm, and was located 51 mm vertically below the cleaned Corning 7059 glass substrates. The bottom Au electrode, of thickness typically 60

nm, was thermally evaporated from a Mo boat. The sputtered films were then deposited in the sputtering system, before evaporated top Au electrodes, of typical thickness 40 nm, were deposited. Sample active areas were 1.2×10^{-5} m^2, allowing deposition of six individual samples on each substrate. After deposition the film thicknesses were measured accurately using a Planer Surfometer SF200 stylus instrument, and were in the range 40 - 160 nm, with deposition rates typically 0.055 nm s^{-1}.

Electrical measurements were performed in a separate evacuated cryostat system. For AC measurements temperatures were controlled in the range 143 - 373 K, and were monitored using a Fluke 52 K/J digital thermometer. For permittivity measurements, and to investigate the class of contacts, capacitance was measured at a fixed standard frequency of 1 kHz using a Hewlett-Packard 4276A LCZ meter equipped with an internal $\pm$ 40 V DC power supply. AC measurements of conductance, capacitance and loss tangent of the samples were also made using the LCZ meter over the frequency range 100 Hz - 20 kHz.

3 Results and discussion

3.1 Permittivity and class of electrodes

The value of the relative permittivity and the type of contacts are important considerations in any metal/insulator structure. The mean value of the relative permittivity is likely to depend on the deposition and substrate parameters, as well as on the source of the material and the electrodes. The type of contact will depend not only on work-function differences between the electrode and insulator material, but also on the presence of and concentration of surface states. Capacitance measurements as functions of voltage level and polarity as well as the thickness dependence of capacitance were used to investigate these properties.

Capacitance was measured as a function of applied voltage for both polarities up to 6 V for a series of samples with thicknesses in the range 50 - 160 nm. For Schottky barrier (blocking) contacts, a depletion region forms at the metal/insulator interface, and the depletion region capacitance C_d depends sensitively on the voltage drop V_j across the junction [23]. In our measurements there was very little dependence of the capacitance on the voltage applied, except for very minor effects for higher electric fields with lower film thickness and higher applied voltages. Since the capacitance was essentially independent of the applied voltage, no appreciable depletion region appeared at the Au electrodes, which then act as ohmic contacts. This behaviour is similar to that observed previously for the case of Al electrodes [18].

For ohmic contacts, the overall capacitance of the structure C is determined by the permittivity of the insulator and by geometric factors. A plot of the capacitance C as a function of the reciprocal thickness $1/d$ should be linear with slope $\varepsilon_r \varepsilon_0 A$, where A is the active area. Fig. 1 shows such a plot of the zero bias capacitance for each of the samples. The gradient yields a value of the permittivity of 6×10^{-11} F m^{-1} (relative permittivity ε_r = 6.8). This value is in reasonable agreement with values found previously by various workers on materials deposited by different methods. In CVD films values of 6.8 [24] and 7-10 [25] were found, the latter depending on the silane/ammonia ratio used. Values of 7.5 were determined using PECVD [26] and 6.0 using electron-cyclotron PECVD at room temperature [20], while values in the range 7-11 were found for films prepared using a glow-discharge [27]. For sputtered films using Al electrodes a lower value of 6.3 has been determined by the present authors [18]. Clearly the value of ε_r

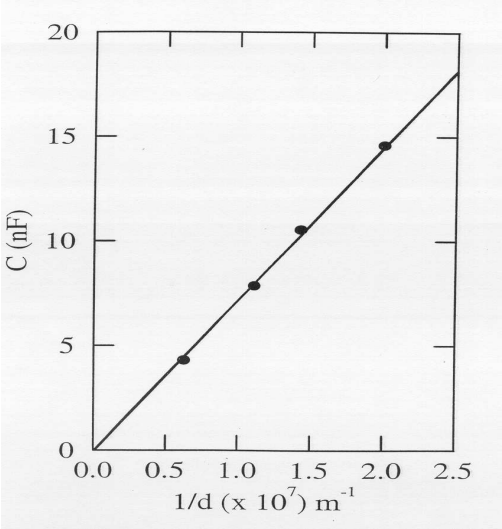

Fig. 1. Dependence of capacitance on reciprocal thickness. The linear dependence implies that the capacitance follows the geometric relationship $C = \varepsilon_r \varepsilon_0 A/d$. The gradient yields a value of permittivity of 6.0×10^{-11} F m^{-1} (relative permittivity 6.8).

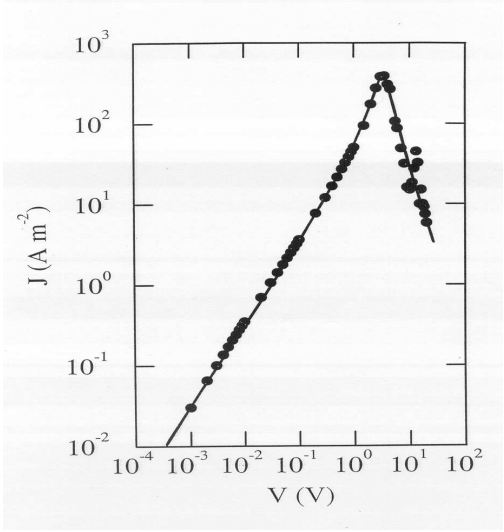

Fig. 2. Dependence of current density on applied voltage for a sample of thickness 40 nm. The VCNR behaviour indicates that the sample has undergone an electroforming process.

depends significantly on the deposition conditions, usually giving a value which is lower than that in the bulk. In sputtered films the type of electrode can also influence the measured value of ε_r, and in the present case this is probably related to the presence of Au in the silicon nitride as discussed in the following section. The value of ε_r = 6.8 determined above was used in the calculations following.

3.2 DC conductivity

A logarithmic plot of the current density J as a function of the applied voltage V is shown in Fig. 2 for a film of thickness 40 nm at room temperature, and clearly implies that the conduction is ohmic up to about 0.1 V. Above this voltage the current increased more rapidly, and above 2 V the current *decreased,* showing current fluctuations, particularly above 10 V. This type of behaviour is typical of samples which have undergone an *electroforming* process, after which voltage-controlled differential negative resistance (VCNR) behaviour is observed. Similar characteristics have also been observed in other insulators [28], and in particular in Au-SiO_x-Au sandwich samples [29]. A low value of the forming voltage $V_F \sim$ 2-5 V was earlier quoted for some oxides and fluorides [28]. Electroforming behaviour is widely thought to involve the field-assisted diffusion of the metal electrode material into the insulator, and the VCNR behaviour is thought to be the result of non-uniform conduction through lower resistivity regions, which progressively cease to conduct as the voltage in increased owing to the effects of Joule heating.

It is clear from this behaviour that electroforming is observed in the present system, as in similar SiO_x samples, which also show Poole-Frenkel conductivity before electroforming [29].

In order to further investigate the behaviour of the present samples before electroforming the maximum voltage applied was restricted to 1.5-2.0 V, below the forming voltage. For four different film thicknesses of 50, 70, 90 and 160 nm, the slopes of all logarithmic $J - V$ curves were approximately unity, and therefore ohmic conduction was followed. In this low voltage region, before the onset of high-field conduction effects, the conduction process was therefore due to thermally-generated carriers, where the current density-voltage relation follows a form of Ohm's law given by

$$J = en_0\mu\frac{V}{d} \tag{1}$$

where n_0 is the concentration of thermally generated electrons in the conduction band, μ is the mobility and d is the silicon nitride thickness. Using $\mu = 5 \times 10^{-12}$ m^2 V^{-1} s^{-1} obtained for sputtered silicon nitride films [18], values of n_0 of 1.80×10^{23} m^{-3}, 4.50×10^{23} m^{-3}, 8.75×10^{23} m^{-3}, and 3.13×10^{24} m^{-3} were found from Eqn. (1) for the samples of thickness 160 nm, 90 nm, 70 nm and 50 nm, respectively. The mean value of n_0 for these four samples is 1.6×10^{24} m^{-3}, which is nearly two orders of magnitude higher than the value obtained in sputtered Al-Si_3N_4-Al structures [18]. This difference is probably related to the use of the Au electrodes in the present case, which are expected to show some penetration into the insulator even at voltages below V_F. The higher carrier concentrations obtained above for the thinner samples tends to support this view.

In order to explore the conduction mechanism taking place before electroforming, the previously mentioned data are plotted in Fig. 3, with log$J$as a function of $V^{1/2}$. There is a clear linear relationship between these variables which is consistent with field-assisted carrier excitation into the conduction band (the Poole-Frenkel effect). In this case the $J-V$characteristic should follow a relationship of the form [30]

$$J = J_0 \exp\left(\frac{\beta_{PF}F^{1/2}}{kT}\right) \tag{2}$$

where k is Boltzmann's constant, T is the absolute temperature, d is the film thickness and J_0 is the low-field current density. β_{PF} is called the Poole-Frenkel field-lowering coefficient, whose theoretical value depends only on the permittivity, and is given by [30]

$$\beta_{PF} = \left(\frac{e^3}{\pi\varepsilon_r\varepsilon_0}\right)^{1/2} \tag{3}$$

Schottky emission at the electrodes which shows similar $J - V$ characteristics [30] is precluded in the present case, since Schottky barriers at the electrode interfaces are ruled out by the capacitance measurements described in Section 3.1. An average value of the field-lowering coefficient $\beta = 1.9 \times 10^{-5}$ eV m$^{1/2}$ V$^{-1/2}$ was determined from the data of Fig. 3, whereas a theoretical value of $\beta_{PF} = 2.9 \times 10^{-5}$ eV m$^{1/2}$ V$^{-1/2}$ is obtained using $\varepsilon_r = 6.8$. However this calculated value may be inappropriate in the present case, since the high-frequency dynamic relative permittivity value of 4-7 should be used [31]. It should also be noted that Yadav and Joshi [32] found experimental values of the field-lowering coefficient considerably smaller than the theoretical

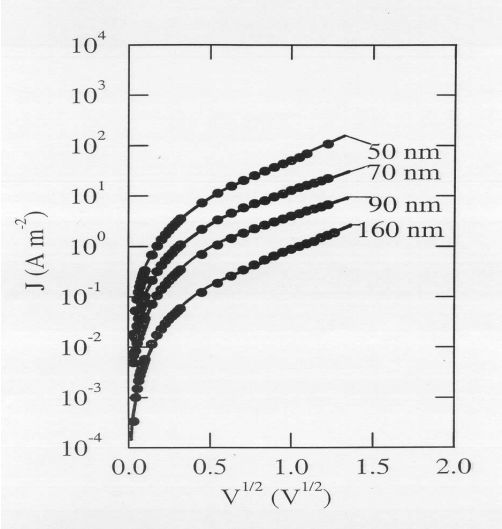

Fig. 3. Dependence of current density on the square root of applied voltage for samples of different thickness before electroforming. The linear dependence indicates that the conductivity is via a field-lowering process, which was identified with the Poole-Frenkel effect.

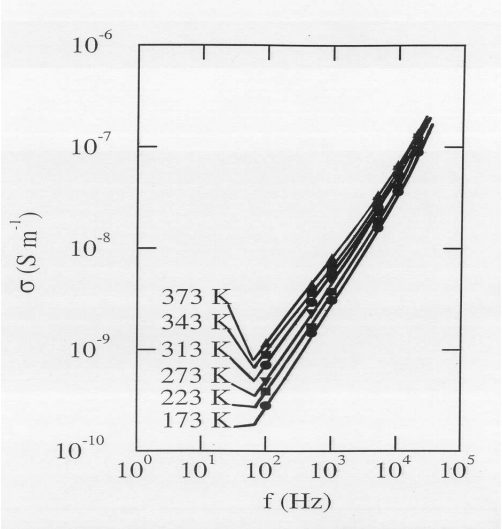

Fig. 4. Dependence of AC conductivity on frequency at temperatures of 173 - 373 K for a sample of thickness 160 nm. The slope s was in the range $0.83 \leq s \leq 1.31$, and is consistent with Elliott's hopping model in the low frequency range, where the density of localised states was estimated to be approximately 10^{24} m^{-3}.

Poole-Frenkel value in ion-beam-synthesized Si_3N_4 films, and that there are several modified versions of Eqn. (2) in the literature to account for the current density variations in the presence of various combinations of centres, including donors and traps. It was therefore concluded that a form of Poole-Frenkel emission is observed in these films as has been observed previously [16,19-22,31], but that the low experimental values of β_{PF} obtained are related to an inexact knowledge of the trapping and donor levels present, and the appropriate value of the relative permittivity.

The use of Au rather than Al electrodes in the present samples is seen to influence the conductivity in several ways, all of which may be accounted for in terms of the penetration of Au atoms into the insulator. At low voltages the ohmic conductivity is increased, at intermediate voltages the high fields stimulate Poole-Frenkel emission at the centres, and at high voltages full electroforming occurs. Thus the Poole-Frenkel conductivity may be associated with the field-assisted diffusion of Au into the insulator, and not with the existence of Si-N bonds, which are also present in samples with Al electrodes where Poole-Frenkel conductivity is absent.

3.3 AC conductivity

Fig. 4 shows the dependence of AC conductivity σ on frequency for different fixed temperatures in the range 173 - 373 K for a film of thickness 160 nm. It is clear from the figure that σ is very

Frequency range	173 K	223 K	273 K	313 K	343 K	373 K
100 Hz - 1 kHz	1.04	0.99	0.98	0.91	0.87	0.83
1 - 10 kHz	1.07	1.03	1.00	0.96	0.95	0.92
10 - 20 kHz	1.31	1.28	1.16	1.07	1.06	1.04

Tab. 1. Dependence of the index $s(T)$ on temperature and frequency range determined from the data of Fig. 4 for a sample of thickness 160 nm.

sensitive to frequency and increases with increasing temperature, although at higher frequencies the dependence on temperature is less marked and there is a tendency for the curves to merge. The relationship between conductivity and angular frequency ω may be described by [33]

$$\sigma = A\omega^{s(T)} \tag{4}$$

where A is a proportionality constant and $s(T)$ is a temperature-dependent index. The index s can be determined from the slope of a logarithmic conductivity-frequency curve [34], i.e.

$$s = \frac{d(\ln \sigma)}{d(\ln \omega)} \tag{5}$$

Mean values of s over three fixed frequency ranges, as calculated from the data of Fig. 4, are presented in Table1 for each temperature. From the table it is evident that s is relatively close to unity, lying in the range $0.83 \leq s \leq 1.31$. Furthermore there is a general tendency for s to decrease with increasing temperature and to increase with increasing frequency, as observed in other dielectric films, notably CeO_2 [35] and SiO_x [36]. These results were interpreted using the hopping model of Elliott [34], where the carriers are considered to hop over a potential barrier between adjacent sites, and the AC conductivity is given by

$$\sigma(\omega) = \frac{\pi^2 N^2 \varepsilon}{24}\left(\frac{8e^2}{\varepsilon W_m}\right)^6 \frac{\omega^s}{\tau_0^\beta} \tag{6}$$

where N represents the density of localised states, ε (=$\varepsilon_r\varepsilon_0$) is the permittivity, τ_0 is the effective relaxation time (approximately 10^{-13} s) [34], and s = 1 - β at low temperature, where β = $6kT/W_m$ and W_m is the optical band gap. Since the maximum value of s permitted by this model is unity it cannot be fully applicable in the present case. However in the related dielectric SiO_x, hopping conduction takes place in which a sublinear dependence of σ on ω is followed at low frequencies, tending towards a square-law at higher frequencies [33,36,37] and a similar process occurs in silicon nitride. An estimate of the density of localised states was obtained from Eqn. (6) using the values of s = 0.99 and $\sigma \sim 3.7 \times 10^{-9}$ S m^{-1} at T = 223 K and f = 1 kHz. Values of $\varepsilon = 6 \times 10^{-11}$ F m^{-1} (Section 3.1) and W_m = 5.3eV for amorphous Si_3N_4 [38], yield a value of $N \sim 10^{24}$ m^{-3}. This in good agreement with the value of $N_t = 2 \times 10^{24}$ m^{-3} for the trap concentration obtained from DC measurements [18]; thus the DC trap concentration corresponds to the AC density of localised states, offering additional evidence for this type of conductivity.

In Fig. 5 the dependence of the conductivity σ on inverse temperature $1/T$ is shown for the same sample as in Fig. 4 for various frequencies in the range 100 Hz - 20 kHz over the

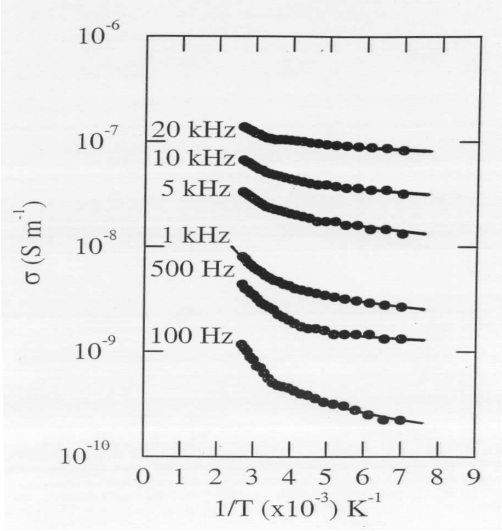

Fig. 5. Dependence of AC conductivity on inverse temperature at frequencies of 100 Hz - 20 kHz for a sample of thickness 160 nm. Activation energies were 0.04 - 0.1 eV above room temperature and 0.006 - 0.01 eV below room temperature, and consistent with a hopping process.

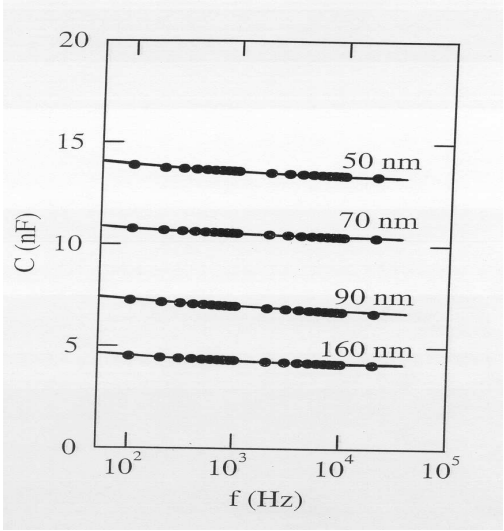

Fig. 6. Dependence of room temperature capacitance on frequency for samples of thickness 50 - 160 nm. The geometric dependence of capacitance, as also evident in Fig. 1, is the major cause of the capacitance variation.

temperature range 143 - 373 K. It is evident from the change in slope of the figure that the conductivity is more sensitive to temperature above room temperature ($1/T \sim 3.4 \times 10^{-3}$ K^{-1}) than below room temperature. Discrete carrier activation energies E may be calculated from the slope of a lnσ - $1/T$ plot such as Fig 5. Although in the present case hopping activation energies are expected to be continuously distributed, such calculations give a good indication of the range of values. Above room temperature the activation energies were in the range 0.04 - 0.1 eV. A hopping conduction process is consistent with this range of activation energies, and is in agreement with earlier results of Sullivan and Card [39] and of Sze [40]. Below room temperature the calculated activation energies were lower, in the range 0.006 - 0.01 eV. There was no evidence of higher activation energies of the order of several tenths of an electron-Volt characteristic of a free-band conduction process, and thus this type of mechanism is absent in samples with Au electrodes.

3.4 Capacitance and loss tangent

Fig. 6 shows the variation of room temperature capacitance C with frequency for samples of thickness 50 - 160 nm. In Fig. 7 the dependence of capacitance on frequency is shown for a sample of thickness 160 nm at different fixed temperatures in the range 143 - 373 K. In general the capacitance increased with increasing temperature, but decreased with increasing frequency. At high frequencies all the capacitances tended towards a constant value of approximately 4.1

nF, irrespective of temperature.

A similar dependence of capacitance on frequency and temperature has previously been observed in the dielectrics CeO_2 [35] and SiO_x [36].These were interpreted in terms of an equivalent circuit model of Goswami and Goswami [41], in which the sandwich structure is modelled by a frequency-independent capacitive element $C^{/}$ in parallel with a temperature-dependent resistance R, and both in series with a constant low-value resistance r which represents the contacts and leads. The resistance R is thermally activated, decreasing with increasing temperature. This model was developed from the model of Simmons *et al* [42], which applies to samples having Schottky-barrier contacts. According to the model of Goswami and Goswami the measured series capacitance C_S is given by the relationship

$$C_S = C^{'} + \frac{1}{\omega^2 R^2 C'} \tag{7}$$

The behaviour shown in Fig. 7 is consistent with this expression, in that the measured capacitance should decrease with increasing frequency, reaching a constant value $C^{/}$ at high frequencies. Similarly, the increase in capacitance with increasing temperature is also predicted, as R decreases with increasing temperature, and the second term on the right-hand side of Eqn. (7) increases.

The dependence of loss tangent, tanδ, on frequency and temperature is shown in Fig.8 for a sample of thickness 160 nm. In general, tanδ initially decreased with increasing frequency, before passing through a minimum and increasing again at higher frequencies. The minimum is not apparent for the lowest temperature, although the theory below suggests that it should appear at a lower frequency than covered experimentally. According to the model, the loss tangent is given by [41]

$$\tan\delta = \frac{\left(1 + \frac{r}{R}\right)}{\omega R C'} + \omega r C' \tag{8}$$

The position of the loss minimum ω_{min} is given by

$$\omega_{min} = \frac{1}{C'\sqrt{rR}} \tag{9}$$

The first term on the right-hand side of Eqn. (8) dominates at low frequencies so tanδ is predicted to decrease with increasing frequency. At higher frequencies the second term dominates, and therefore tanδ should increase with increasing frequency. This behaviour is clearly apparent in Fig.8. Furthermore the position of ω_{min} appears to shift to higher frequencies for increasing temperatures, as also predicted by Eqn. (9), since R decreases with increasing temperature.

4 Summary and conclusions

Capacitance-voltage-thickness measurements indicate that the Au/silicon nitride contact is ohmic and that $\varepsilon_r \sim 6.8$, exceeding the value of 6.3 found in similar samples having Al electrodes. The differing values were related to the possible presence of the Au electrode material in the silicon nitride layers. Samples initially showed ohmic conductivity with a mean carrier concentration of

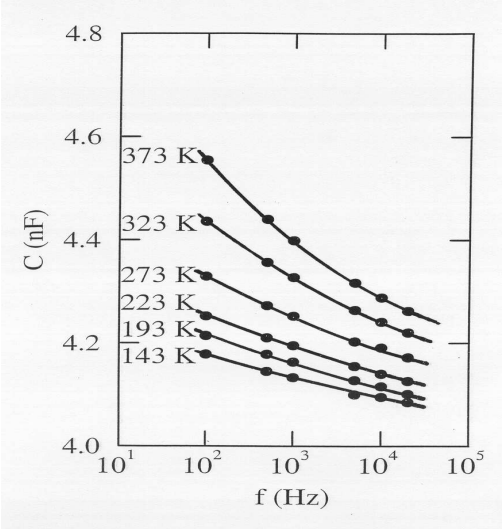

Fig. 7. Dependence of capacitance on frequency at temperatures of 143 - 373 K for a sample of thickness 160 nm. At higher frequencies the capacitance tends towards 4.1 nF irrespective of temperature, consistent with the model of Goswami and Goswami.

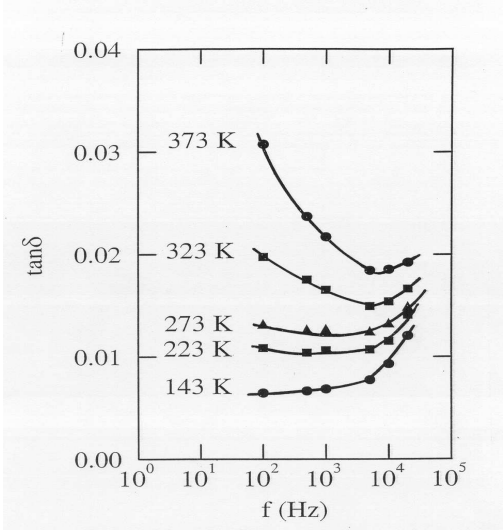

Fig. 8. Dependence of loss tangent on frequency at temperatures of 143 - 373 K for a sample of thickness 160 nm. The observed minimum, which shifts to higher frequencies at higher temperatures, is also consistent with the model of Goswami and Goswami.

about 1.6×10^{24} m^{-3} which is higher than in samples with Al electrodes, reflecting the presence of additional centres within the silicon nitride layers. At higher voltages Poole-Frenkel conductivity was identified having a typical value for the Poole-Frenkel field-lowering coefficient of $\beta_{PF} = 1.9 \times 10^{-5}$ eV m$^{1/2}$ V$^{-1/2}$, which is significantly lower than the theoretical value. This may be related to the fact that the exact nature of the energy levels appearing within the band-gap of the silicon nitride films is undetermined and that the high frequency optical relative permittivity is more likely to be applicable than the low frequency value. Further work on identifying the donor and trap levels present, using for instance thermally stimulated current measurements, is probably necessary to resolve this question. At voltages above 2 V there was evidence of VCNR and electroforming behaviour as previously observed in other insulating films having Au electrodes. AC activation energies were low and consistent with a hopping conduction process. The value of the exponent s derived from conductivity-frequency data was always less than 2, and therefore also consistent with a hopping process. Values of the density of localised states estimated from Elliott's model in its region of applicability, were consistent with earlier DC measurements of trap concentrations. The dependence of the dielectric properties on frequency and temperature were in agreement with the model of Goswami and Goswami for dielectric films with ohmic contacts, and typical of that shown by some other amorphous materials.

It has been shown that although sputtered silicon nitride films share some features of their electrical conductivity with PECVD and LPCVD films there are also significant differences. The

principal novelty of the results reported is that such films exhibit Poole-Frenkel conductivity with Au electrodes, but not with Al electrodes. This suggests that the Poole-Frenkel centres are associated with penetration of Au into the insulator, and not with Si-N bonds as has been recently reported in hydrogenated amorphous silicon nitride and oxynitride films prepared by PECVD [43].

Acknowledgement: S.A. Awan wishes to acknowledge the financial support of Peshawar University, Pakistan, from its own resources throughout her three years of postgraduate study at Keele University, U.K. R.D. Gould wishes to thank the organising committee of the Solid State Surfaces and Interfaces III conference for inviting him to present this paper.

References

[1] V. Kapoor, R.S. Baily, H.J. Stein, J. Vac. Sci. Technol. A 1 (1993) 600.

[2] A. Malik, X.W. Wang, T.P. Ma, G.J. Cui, T. Tamagawa, B.L.Halpen, J.J. Schmitt, J. Appl. Phys. 79 (1996) 8507.

[3] K.-M. Chang, J.-Y. Tsai, C.-H. Li, T.-H. Yeh, S.-W. Wang, J.-Y. Yang, J. Appl. Phys. 79 (1996) 8503.

[4] D.G. Park, M. Tao, D. Li, A.E. Botchkarev, Z. Fan, Z. Wang, S.N. Mohammed, A. Rockett, J.R. Abelson, H. Morkoç, A.R. Heyd, S.A. Alterovitz, J. Vac. Sci. Technol. B. 14 (1996) 2674.

[5] J.A. Amick, G.L. Schnoble, J.L. Vossen, J. Vac. Sci. Technol. 14 (1977) 1053.

[6] J.R. Elmiger, M. Kunst, Mater. Res. Soc: Symp. Proc. 426 (1996) 129.

[7] R. Kishore, S.N. Singh, B.K. Das, Infrared Phys. Technol. 38 (1997) 83.

[8] J.M. Lopez-Villages, A. Garrido, M.S. Bertran, A. Canillas, J.R. Morante, Mater. Res. Soc: Symp. Proc. 258 (1992) 655.

[9] J.R. Elmiger, R. Schieck, M. Kunst, J. Vac. Sci. Technol. A 15 (1997) 2418.

[10] H. Fritzsche, Appl. Phys. Lett. 65 (1994) 2824.

[11] G. Rieder, F. Olcaytug, Thin Solid Films 89 (1982) 95.

[12] E. Paloura, K. Nauka, J. Lagowski, H.C. Gatos, Appl. Phys. Lett. 49 (1986) 97.

[13] T.P. Ma, IEEE Trans. Electron. Devices 45 (1998) 680.

[14] C. Ye, Z. Ning, M. Shen, H. Wang, Z. Gan, Appl. Phys. Lett. 71 (1997) 336.

[15] F. Martin, X. Aymerich, Thin Solid Films 221 (1992) 147.

[16] S.W. Hseih, C.Y. Chang, Y.S. Lee, C.W. Lin, S.C.Hsu, J. Appl. Phys. 76 (1994) 3645.

[17] V.T. Volkov, F. Sdtunkina, Thin Solid Films 247 (1994) 145.

[18] S.A. Awan, R.D. Gould, S. Gravano, Thin Solid Films 355/356 (1999) 456.

[19] H. Lorentz, I. Eisele, J. Ramm, J. Edlinger, M. Bühler, J. Vac. Sci. Technol. B 9 (1991) 208.

[20] Y.-C. Jeon, H.-Y. Lee, S.-K. Joo, J. Appl. Phys. 75 (1994) 979.

[21] E.C. Paloura, J. Lagowski, H.C. Gatos, J. Appl. Phys. 69 (1991) 3995.

[22] M. Tao, D. Park, S.N. Mohammad, D. Li, A.E. Botchkerav, H. Morkoç, Phil. Mag.B 73 (1996) 723.

[23] S.M. Sze, Physics of Semiconductor Devices, Wiley, New York, 2nd edn., 1981, p. 249.

[24] L. Popova, B.Z. Antov, P.K. Vitanov, Thin Solid Films 36 (1976) 157.

[25] G.A. Brown, W.C. Robinette, H.G. Carlson, J. Electrochem. Soc: Solid State Sci. 115 (1968) 948.

[26] G.N. Parsons, J.H. Souk, J. Batey, J. Appl. Phys. 70 (1991) 1553.

[27] R.C.G. Swann, R.R. Mehta, T.P. Cauge, J. Electrochem. Soc: Solid State Sci. 114 (1967) 713.

[28] A.K. Ray, C.A. Hogarth, Int. J. Electron. 57 (1984) 1.
[29] R.D. Gould, M.G. Lopez, Thin Solid Films, 343/344 (1999) 94.
[30] J.G. Simmons, J. Phys. D: Appl. Phys. 4 (1971) 613.
[31] S.M. Sze, J. Appl. Phys. 38 (1967) 2951.
[32] A.D. Yadav, M.C. Joshi, Thin Solid Films 102 (1983) 187; corrigendum Thin Solid Films 103 (1983) L49.
[33] N.F. Mott, E.A. Davis, Electronic Processes in Non-Crystalline Materials, Clarendon Press, Oxford, 1971.
[34] S.R.Elliott, Phil. Mag. 36 (1977) 1291.
[35] Z.T. Al-Dhhan, C.A. Hogarth, Int. J. Electron. 63 (1987) 707.
[36] M.G. Lopez, R.D. Gould, Thin Solid Films 254 (1995) 291.
[37] F. Argall, A.K. Jonscher, Thin Solid Films 2 (1968) 185.
[38] J. Robertson, Phil. Mag. B 69 (1994) 307.
[39] L. Sullivan, H.C. Card, J. Phys. D: Appl. Phys. 7 (1974) 1531.
[40] S.M. Sze, J. Appl. Phys. 38 (1967) 2951.
[41] A. Goswami, A.P. Goswami, Thin Solid Films 16 (1973) 175.
[42] J.G. Simmons, G.S. Nadkarni, M.C. Lancaster, J. Appl. Phys. 41 (1970) 538.
[43] H. Kato, H. Sato, Y. Ohki, K.S. Seol, T. Noma, J. Phys: Condens. Matter 15 (2003) 2197.